Spatially separating the conformers of the dipeptide Ac-Phe-Cys-NH_2

Nicole Teschmit,[1,2,3] Daniel A. Horke,[1,2] and Jochen Küpper[1,2,3,4,*)]

[1)] *Center for Free-Electron Laser Science, Deutsches Elektronen-Synchrotron DESY, Notkestrasse 85, 22607 Hamburg, Germany*

[2)] *The Hamburg Center for Ultrafast Imaging, Universität Hamburg, Luruper Chaussee 149, 22761 Hamburg, Germany*

[3)] *Department of Chemistry, Universität Hamburg, Martin-Luther-King-Platz 6, 20146 Hamburg, Germany*

[4)] *Department of Physics, Universität Hamburg, Luruper Chaussee 149, 22761 Hamburg, Germany*

(Dated: 1 June 2018)

Atomic-resolution-imaging approaches for single molecules, such as coherent x-ray diffraction at free-electron lasers, require the delivery of high-density beams of identical molecules. However, even very cold beams of biomolecules typically have multiple conformational states populated. We demonstrate the production of very cold ($T_{\mathrm{rot}} \sim 2.3$ K) molecular beams of intact dipeptide molecules, which we then spatially separate into the individual populated conformational states. This is achieved using the combination of supersonic expansion laser-desorption vaporisation with electrostatic deflection in strong inhomogeneous fields. This represents the first demonstration of a conformer-separated and rotationally-cold molecular beam of a peptide, and will enable future single biomolecule x-ray diffraction measurements.

Proteins are the workhorses of biological functionality in living cells and are at the heart of, for instance, the transport of oxygen, the catalysis of biochemical reactions and interactions, or the reproduction of cells and replication of DNA. This wide-ranging functionality is enabled by the unique and specific 3-dimensional (3D) structures of these systems. While every protein is composed of a sequence of the 20 amino acids encoded in RNA, the exact sequence and resulting intra-molecular interactions lead to a specific and unique 3D structure, determining a proteins functionality. Changes in this 3D structure, such as misfolding, can dramatically alter protein function with potentially wide-ranging consequences, such as neurodegenerative diseases.[1–3] Especially the strong hydrogen bonding between amino acids within the sequence has a profound effect on the resulting protein structure.[4–7] In order to study the underlying intramolecular and hydrogen-bonding interaction in detail, one often turns to studying isolated small peptide fragments in the gas-phase.[8–12] However, even single amino acids and dipeptides often populate several conformational states,[7,13–16] e. g., rotational structural isomers, complicating detailed analysis and the extrapolation from small model data to entire protein complexes. Mapping the structure-function relationship of these biomolecular machines thus requires reproducible samples in the gas-phase in well-defined initial states.[17–20] More generally, species- and conformer-pure samples of peptides in the gas-phase would open the door for novel non-species-specific experimental techniques, such as atomic-resolution diffractive imaging with x-rays[21–25] or electrons,[26,27] attosecond-electron-dynamics experiments,[28] or kinetic studies of the chemical reactivity of a single conformer.[18] Such experiments inherently do not distinguish which conformer was probed, making it very difficult or even impossible to interpret data collected with more than one conformer present in the interaction volume.

To investigate biomolecules in the gas-phase requires their vaporisation without fragmentation or ionisation. Laser desorption (LD) has been demonstrated as a technique to vaporise such thermally labile molecules,[29,30] and the combination with supersonic expansion allows for rapid cooling of the desorbed molecules.[30–33] However, even in such cold molecular beams different conformers, which differ by rotations about single bonds, can coexist. In order to produce a pure beam containing only a single conformer, we combine LD with electrostatic deflection.[34] This allows the spatial separation of molecular species based on their distinct interaction with the applied electric field. This so-called Stark effect is dependent on the quantum-state-specific effective dipole moment and this technique has been demonstrated to spatially separate conformers of small aromatic molecules,[35,36] and for very small molecules it can even produce single-quantum-state samples.[37–39] Furthermore, due to the rotational-state-dependence of the Stark effect,[34,40,41] deflection allows the creation of very cold ($T_{\mathrm{rot}} < 100$ mK) molecular ensembles. This can significantly improve the degrees of laser alignment and mixed-field orientation of molecules in space[42] and thus enable ensemble-averaged single-molecule imaging.[24,43]

Here, we present the first combination of laser desorbed biomolecules with electrostatic deflection and demonstrate the spatial separation of the two main conformers of the dipeptide Ac-Phe-Cys-NH_2, shown in Figure 1 a. These two conformers differ in their hydrogen-bonding interactions and, hence, 3D structure. One conformer, indicated by red colour throughout the paper, forms a hydrogen bond from the SH group to the oxygen on the carboxamide group, while the other conformer, blue colour, forms a hydrogen bond from the SH to the delocalised π-system. These two "beautiful molecules"[44] have been previously identified using vibrational and electronic spectroscopy.[16,45] In a cold molecular beam these two conformers cannot interconvert, however, their significantly

*)Electronic mail: jochen.kuepper@cfel.de; https://www.controlled-molecule-imaging.org

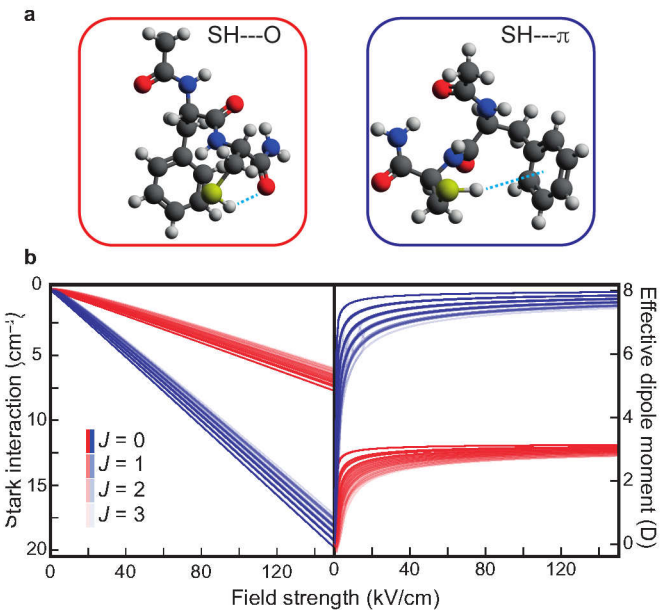

FIG. 1. a: The two main conformers of the dipeptide Ac-Phe-Cys-NH_2 with their distinct hydrogen-bonding interactions of the cystine sidechain indicated. b: The Stark energy curves (left) and effective dipole moments (right) for the lowest rotational states of the two conformers.

different dipole moments of 3.2 D and 8.1 D result in different Stark interactions, see Figure 1 b. This allows for their spatial separation with the electrostatic deflector if a sufficiently cold molecular ensemble can be created.[34] This would, furthermore, also separate the sample of interest from unwanted fragments or contaminants present in the beam, such as carbon clusters from the LD process.[33] Compared to the separation of molecular ions in ion mobility measurements,[46,47] our method enables the separation of neutral species, avoiding space-charge density limitations that severely affect diffractive-imaging experiments.[25,26] Furthermore, the low temperatures of the generated molecular ensembles allow for strongly fixing the molecules in space[42] — two prerequisites for the recording of atomically resolved molecular movies.[23,24]

RESULTS AND DISCUSSION

Our implementation of the combination of LD with electrostatic deflection is shown schematically in Figure 2; details are given in *Methods*. Briefly, the laser-desorbed molecular beam enters a 15 cm long deflector sustaining electric field strengths on the order of 150 kV/cm^{-1}. The different conformers experience a different vertical deflection within this field, which originates from the Stark-effect interaction between the molecules' space-fixed dipole moment μ_{eff}, Figure 1 b, and the applied electric field ϵ. This leads to a force $\vec{F} = -\mu_{\text{eff}}(\epsilon) \cdot \vec{\nabla}\epsilon$ acting on the molecules.[34,41] Thus, the observed deflection depends

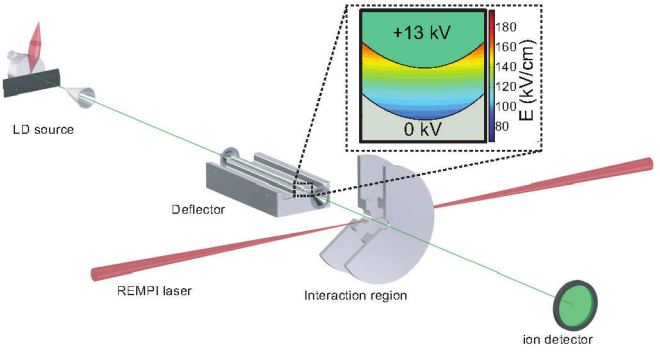

FIG. 2. Schematic of the experimental setup combining the laser desorption (LD) with electrostatic deflection. The inset shows a cross-section of the deflector and the electric-field strength inside.

on the effective-dipole-moment-to-mass ratio and the two conformers experience different forces, i. e., transverse accelerations, in the electric field, leading to their spatial separation. The molecular beam and the separation of conformers was characterised by recording spatial profiles of the beam. This was achieved by vertically translating the ionisation laser beam through the horizontal molecular beam, and recording the relative density as a function of laser height. The ionisation laser was tuned to specific resonances to selectively detect a single conformer.

Such spatial molecular beam profiles for the individual conformers in the absence of an electric field, i. e., with the deflector at 0 kV, are shown in Figure 3 a, to which all beam-profile intensities have been normalised. These show that both conformers are centered around $y = 0$ mm and exhibit the same spatial distribution. The measured width of the molecular beam is predominately defined by the apertures of skimmers and the electrostatic deflector placed in the molecular beam, see *Methods*. The relative population of the two conformers in the beam was assessed by placing the ionisation laser focus at the center of the profile, as indicated by the black arrow in Figure 3 a, and scanning the ionisation wavelength across the electronic-origin transitions of the two conformers around 37325 cm^{-1} and 37450 cm^{-1}, respectively. The resulting resonance-enhanced multiphoton-ionisation (REMPI) spectrum is shown in Figure 3 d and yielded an intensity ratio of $\sim$2 : 1 for the SH–O and SH–π bound conformers, respectively. Assuming identical ionisation probabilities for the REMPI process, this ratio can be taken as a measure of the relative conformer populations in the molecular beam.

Charging of the electrostatic deflector lead to deflection of the molecular beam in the positive, upward direction, as shown in Figure 3 b,c. Application of 4 kV to the deflector, Figure 3 b, lead to a clear shift of both spatial profiles, with the more polar SH–π-bound conformer shifting significantly more. This created an area, between $\sim$1.7–2.5 mm, were a highly enriched sample of this conformer was obtained, as confirmed by the REMPI

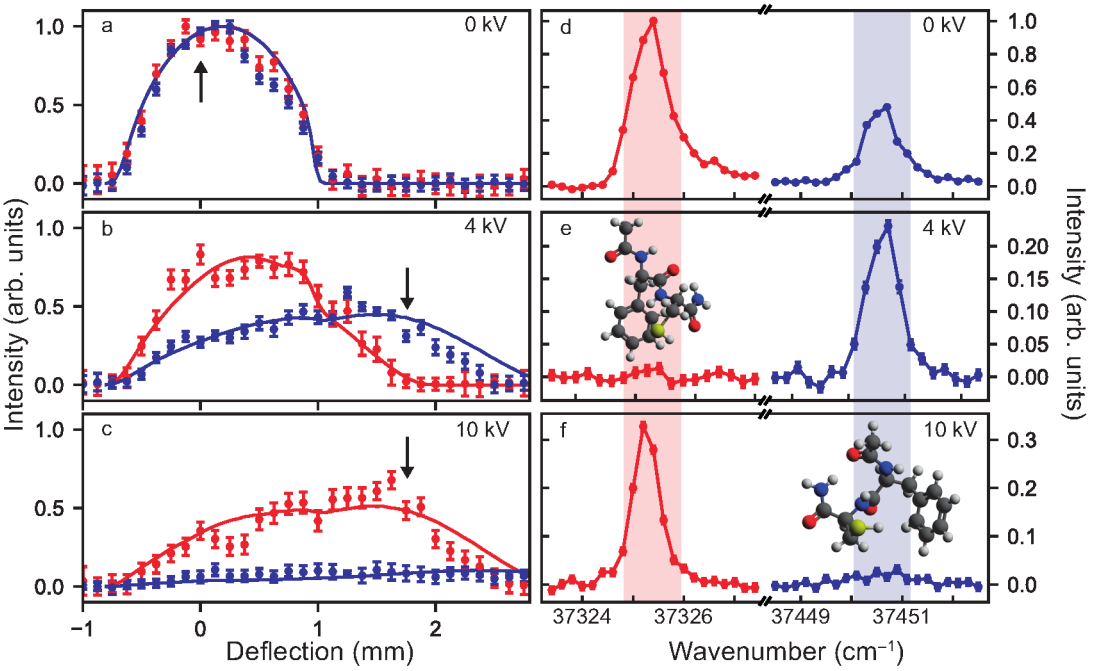

FIG. 3. Spatial molecular beam profiles (a–c) and corresponding REMPI spectra (d–f) for the two main conformers of Ac-Phe-Cys-NH_2. These are collected at deflector voltages of 0 kV (a,d), 4 kV (b,e) and 10 kV (c,e). Solid lines in the deflection profile plots (a–c) are taken from quantum-state resolved trajectory simulations with a 2.3 K thermal state weighting. REMPI spectra are taken at the spatial position indicated by the black arrow in the spatial profiles.

spectrum collected at position $y = 1.75$ mm and shown in Figure 3 e. To separate and create a pure sample of the SH–O-bound conformer, a voltage of 10 kV was applied, leading to depletion of the SH–π-bound system from the interaction region, as shown in Figure 3 c. This is due to the large deflection experienced by this more polar conformer, such that these molecules collided with the deflector or following apertures and no clear beam was observable anymore. Instead, a position-independent small background signal was present. A REMPI spectrum recorded in the deflected beam is shown in Figure 3 f, confirming the highly-enriched sample of the SH—O-bound conformer created under these conditions.

Using a calibrated ion detector, we estimated the number of ions produced per laser shot to be ~1 for REMPI ionisation. By using more efficient strong-field ionisation (SFI) we extracted a lower limit for the absolute number density of 10^7 cm^{-3}, see appendix A for details. Derivation of this density assumes an ionisation efficiency of 1 for SFI and only takes into account the major assigned fragmentation channels for Ac-Phe-Cys-NH_2[33] and thus strictly represent a lower limit of the density.

Further to the deflection of the molecular beam, we observed a significant broadening of the spatial profiles. This is due to the dispersion of the different rotational states in the electric field, arising from the rotational-state-dependence of the Stark effect.[34,41] This is shown in Figure 1 b for $J = 0 \ldots 3$ states, indicating the larger effective dipole moment of lower-lying rotational states, leading to these states being deflected more, and hence the creation of a rotationally colder sample in the deflected beam.[23,40] To extract approximate rotational temperatures and quantum-state distributions in the deflected beam, we have simulated particle trajectories through our setup for the different populated rotational states,[34] details are given in appendix B. Resulting simulated deflection profiles are shown as solid lines in Figure 3 a–c, which were obtained by applying a thermal-distribution weighting to the individual-state simulations, corresponding to the rotational temperature distribution from our LD-molecular-beam source. We extract an approximate rotational temperature of 2.3±0.5 K for the laser-desorbed molecular beam.

Furthermore, we extract the quantum-state distribution within the deflected beam in Figure 3 e,f. These are shown in Figure 4 and indicate that the deflector creates a significantly colder ensemble. While this has a non-thermal rotational state distribution, the highest rotational states populated are approximately corresponding to a 1.5 K distribution. Even colder ensembles can be probed by moving the interaction region further into the deflected beam, this is indicated by the magenta and cyan distributions in Figure 4, evaluated at position 2.2 mm in the deflected beam, which are comparable to a 1.0 K average.

These results highlight the quantum-state-sensitivity of the electrostatic-deflection technique, allowing us to control conformer populations and rotational state distri-

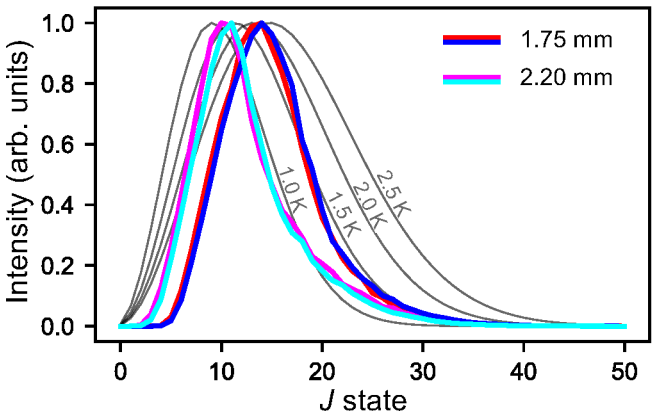

FIG. 4. Relative population of rotational states in the molecular beam for the conformer-pure samples at two deflected positions, 1.75 mm (as in Figure 3) and 2.2 mm. Shown in grey are thermal distributions at various temperatures, as indicated. The red/magenta and blue/cyan lines indicate distributions for the SH–O and SH–π conformer, respectively.

butions within the interaction region and creating samples well-suited for further control techniques such as alignment and orientation.[23,42,48] Moreover, ultrafast imaging experiments benefit from the significantly, typically several orders of magnitude, reduced density of carrier gas in the interaction region, which does not experience deflection in the electric field.

The presented approach is generally applicable to any polar molecule that can be vaporised by laser desorption and entrained in a molecular beam. The achievable degree of species separation depends crucially on the difference in dipole-moment-to-mass ratio,[34,49] and for small peptide systems we estimate that a difference of ∼20 % is sufficient for creating pure samples of the more polar species, whereas differences above ∼50 % should allow creation of a pure sample of either species, with improved setups enabling the separation for even smaller differences.[50,51] The main limitation here is the creation of initially rotationally-cold samples in the desorption and entrainment process, such that an appreciable fraction of population is in the lower lying rotational states that exhibit the largest Stark shift. If this can be further improved, for example through the use of specially designed and higher pressure supersonic expansion valves,[52] higher state purities or the separation of species with smaller dipole-moment differences will be achievable.

CONCLUSION

We demonstrated the combination of laser desorption for the vaporisation of labile biological molecules with the electric deflector for the spatial separation of conformational states and the creation of pure and rotationally-cold samples of individual conformers. Using the prototypical (di)peptide Ac-Phe-Cys-NH_2 as a model system, we showed that its two conformers, in the gas-phase, can be spatially separated and samples of either conformer can be obtained. The measured deflection was quantitatively understood using trajectory calculations, which furthermore allowed us to assign a rotational temperature of 2.3 ± 0.5 K for the beam from our laser desorption source. The generally good agreement between experiment and simulation also confirms the calculated dipole moments and that Stark effect calculations based on the rigid-rotor approximation are sufficient even for these large systems.[53]

The created molecular samples will enable novel x-ray diffractive imaging experiments: they are conformer-pure beams that are well-separated from carrier gas and rotationally cold enough for strong laser alignment and orientation. The achieved densities of around 10^7 cm^{-3} are sufficient for high-resolution diffraction experiments at free-electron laser sources such as the European XFEL, which will deliver up to 26,000 pulses per second, allowing fast collection of data. This enables the collection of a diffraction image within 1 h,[24] and simulated aligned-molecule diffraction patterns for the two conformers, showing marked differences, are shown in appendix C. Our laser desorption source, with its low overall repetition rate, but reasonably long gas pulses of 100s of µs,[33] is well-suited to the pulse-train structure of superconducting-LINAC-based XFELs.[54] The produced rotationally cold samples are well suited to strong-field alignment, which can be achieved using the available in-house laser systems available at FELs.[55]

Our developed technique will more generally enable experiments on conformer-selected biological molecules with inherently non-species-specific experimental techniques, such as (sub-)femtosecond dynamics,[28] reactive collision studies,[18] or diffractive imaging.[25] This will open new pathways to study the intrinsic structure-function relationship of these basic molecular building blocks of the complex biochemical machinery.

METHODS

A laser desorption source, described in detail elsewhere,[33] is used to vaporise the dipeptide Ac-Phe-Cys-NH_2 (APCN, 95% purity, antibodies-online GmbH), which is used without further purification. The resulting cold supersonic molecular beam is skimmed twice before entering the strong inhomogeneous field of the electrostatic deflector: once by a 2 mm skimmer (Beam Dynamics Inc. Model 50.8) 75 mm downstream of the expansion, and again by a 1 mm skimmer (Beam Dynamics Inc. Model 2) 409 mm downstream of the expansion. Within the strong inhomogeneous electric field of the deflector, molecules are dispersed according to their effective dipole moment-to-mass-ratio.[34] The molecular beam is skimmed once more with a 1.5 mm skimmer (Beam Dynamics Inc. Model 2) prior to entering the interaction region. This skimmer can be translated

in height to ensure no part of the molecular beam is cut off. During measurements, data is collected for two skimmer positions and subsequently combined by keeping the highest intensity measured. The relative density of the conformers is probed via resonance-enhanced multi-photon ionisation (REMPI).[16] The ultraviolet probe light is produced by frequency doubling the output of a dye laser (Radiant Dyes NarrowScan, using Coumarin 153 dye in methanol), pumped by the third harmonic of a Nd:YAG laser (Innolas, SpitLight 600). Typical laser-pulse energies were around 19 µJ loosely focused to a 100 µm spot in the interaction region.

The structures and dipole moments of Ac-Phe-Cys-NH_2 were calculated using the GAMESS software suite[56] using the B3LYP functional with a 6-311(p) basis set and confirmed against published structures.[16]

Acknowledgments

We thank Christof Weitenberg and the group of Klaus Sengstock for support with the wavemeter and Thomas Kierspel for the simulation of x-ray diffraction patterns.

This work has been supported by the European Research Council under the European Union's Seventh Framework Programme (FP7/2007-2013) through the Consolidator Grant COMOTION (ERC-614507-Küpper), by the excellence cluster "The Hamburg Center for Ultrafast Imaging – Structure, Dynamics and Control of Matter at the Atomic Scale" of the Deutsche Forschungsgemeinschaft (CUI, DFG-EXC1074), and by the Helmholtz Gemeinschaft through the "Impuls- und Vernetzungsfond". We gratefully acknowledge a Kekulé Mobility Fellowship by the Fonds der Chemischen Industrie (FCI) for Nicole Teschmit.

Appendix A: Determination of a lower limit of the number density

For the density determination a time-of-flight mass spectrum using strong-field ionisation by femtosecond laser pulses (800 nm central wavelength, 40 fs duration, typical pulse energies of 100 µJ) is recorded.[33] In the time-of-flight mass spectrum all peaks originating from the Ac-Phe-Cys-NH_2 molecule are integrated and the total ion current on the detector determined. This is compared to the known calibrated current for a single ion hit, which leads to approximately 18 ions/shot in the $\omega_0 = 50$ µm focus of the laser. Assuming an ionisation efficiency of 1 for strong-field ionisation and a molecular-beam width of 1 mm, this yields a density of 9 x 10^6 cm^3.

Appendix B: Numerical simulations and temperature determination

Spatial molecular-beam profiles were simulated by first calculating the Stark energies for each conformer for all rotational states up to $J = 50$, including all states up to $J = 70$ in the calculation, using the freely available `CMIstark` software package.[41] Rotational constants and dipole moment vectors were taken from the DFT calculations and are summarized in Table A1. Subsequently, for molecules in each quantum state we carried out classical trajectory simulations through the experimental setup, taking into account apertures and applying the appropriate forces when molecules are within the electrostatic deflector.[34] Finally, histograms of the final particle-position densities were determined at the interaction point and the contributions from each quantum state weighted by a Maxwell-Boltzmann distribution for a given initial temperature.[40] Simulated intensities for given conditions – species and deflector voltage – were scaled with a single amplitude-scaling factor to compare with experimental data to account for additional losses and detection efficiency in the setup. The temperature that best described the experimental observations was determined by comparing the combined residuals, that is the absolute deviation between simulation and data, from all deflected data sets, excluding the SH—π conformer at 10 kV where only a

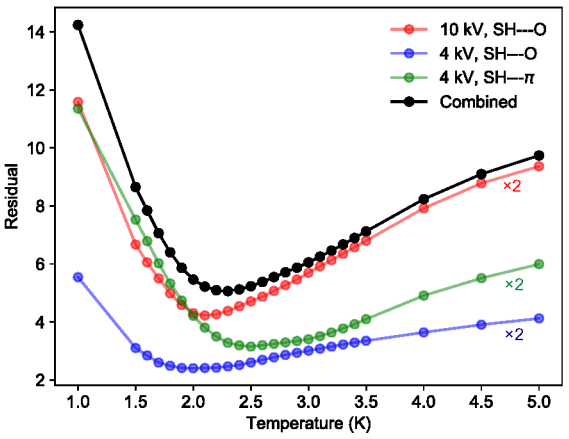

FIG. A5. Residuals from fitting deflection profiles for different voltages and conformers as a function of temperature. Data for the SH—π conformer at 10 kV are not shown as only a constant background was observed. The sum of these residuals (black line) yielded a rotational temperature of 2.3 K.

	SH—O isomer	SH—π isomer
A (Mhz)	340.181593	345.067516
B (MHz)	203.443113	215.965933
C (MHz)	159.877010	175.850323
μ_A (D)	0.768	6.789
μ_B (D)	2.406	-2.701
μ_C (D)	1.975	3.406

TABLE A1. Rotational constants and dipole moment vectors used for calculating the Stark effect.

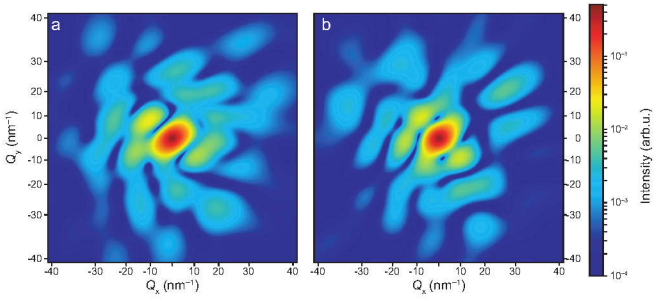

FIG. A6. Simulated x-ray-diffraction patterns of the two conformers of Ac-Phe-Cys-NH_2.

constant low background was observed experimentally, for different rotational temperatures. These are shown in Figure A5 and from the combined residuals (black trace) a rotational temperature of 2.3 K for our molecular beam was extracted. Since the minima for individual deflection profiles deviate by ∼0.5 K, conservative error bounds for the rotational temperature are ±0.5 K.

Appendix C: Simulated X-Ray diffraction patterns

Simulated x-ray diffraction patterns at 9.5 keV photon energy,[25,57] achievable at current XFEL sources such as LCLS and the European XFEL, for the two conformers of Ac-Phe-Cys-NH_2 are shown in Figure A6. The simulation assumes a detector distance of 80 mm and maximum scattering angle on the detector of 50.2 °, corresponding to a resolution of $d \approx 154$ pm at the edge. These calculations assume perfectly aligned molecules and no contribution from background gas in the interaction region, with the most-polarizable axis of the molecules aligned vertically and the second-most-polarizable axis aligned horizontally within the image plane, as it would be obtained in a typical aligned-molecule-diffraction experiment.[25,55,57] A clear, detectable difference between the two patterns is visible. Utilizing the 10 Hz bunch-structure of the upcoming European XFEL will enable the recording of such patterns as well as the reaction path of conformer interconversion.[24]

[1] C. Soto, "Unfolding the role of protein misfolding in neurodegenerative diseases," Nat. Rev. Neurosci. **4**, 49–60 (2003).

[2] K. Hsiao, H. F. Baker, T. J. Crow, M. Poulter, F. Owen, J. D. Terwilliger, D. Westaway, J. Ott, and S. B. Prusiner, "Linkage of a prion protein missense variant to Gerstmann–Sträussler syndrome," Nature **338**, 342–345 (1989).

[3] M. Bucciantini, E. Giannoni, F. Chiti, F. Baroni, L. Formigli, J. Zurdo, N. Taddei, G. Ramponi, C. M. Dobson, and M. Stefani, "Inherent toxicity of aggregates implies a common mechanism for protein misfolding diseases," Nature **416**, 507–511 (2002).

[4] A. R. Fersht, J.-P. Shi, J. Knill-Jones, D. M. Lowe, A. J. Wilkinson, D. M. Blow, P. Brick, P. Carter, M. M. Y. Waye, and G. Winter, "Hydrogen bonding and biological specificity analysed by protein engineering," Nature **314**, 235–238 (1985).

[5] E. S. Feldblum and I. T. Arkin, "Strength of a bifurcated H bond," PNAS **111**, 4085–4090 (2014).

[6] N. S. Nagornova, T. R. Rizzo, and O. V. Boyarkin, "Interplay of intra- and intermolecular H-bonding in a progressively solvated macrocyclic peptide." Science **336**, 320–323 (2012).

[7] B. C. Dian, A. Longarte, and T. S. Zwier, "Conformational dynamics in a dipeptide after single-mode vibrational excitation," Science **296**, 2369–2373 (2002).

[8] E. G. Robertson and J. P. Simons, "Getting into shape: Conformational and supramolecular landscapes in small biomolecules and their hydrated clusters," Phys. Chem. Chem. Phys. **3**, 1–18 (2001).

[9] M. S. de Vries and P. Hobza, "Gas-phase spectroscopy of biomolecular building blocks," Annu. Rev. Phys. Chem. **58**, 585–612 (2007).

[10] A. M. Rijs, G. Ohanessian, J. Oomens, G. Meijer, G. von Helden, and I. Compagnon, "Internal proton transfer leading to stable zwitterionic structures in a neutral isolated peptide," Angew. Chem. Int. Ed. **49**, 2332–2335 (2010).

[11] R. Weinkauf, J. Schermann, M. S. de Vries, and K. Kleinermanns, "Molecular physics of building blocks of life under isolated or defined conditions," Eur. Phys. J. D **20**, 309–316 (2002).

[12] K. Schwing and M. Gerhards, "Investigations on isolated peptides by combined IR/UV spectroscopy in a molecular beam – structure, aggregation, solvation and molecular recognition," Int. Rev. Phys. Chem. **35**, 569–677 (2016).

[13] R. D. Suenram and F. J. Lovas, "Millimeter wave spectrum of glycine - a new conformer," J. Am. Chem. Soc. **102**, 7180–7184 (1980).

[14] M. Y. Choi and R. E. Miller, "Four tautomers of isolated guanine from infrared laser spectroscopy in helium nanodroplets," J. Am. Chem. Soc. **128**, 7320–7328 (2006).

[15] S. Blanco, M. E. Sanz, J. C. Lopez, and J. L. Alonso, "Revealing the multiple structures of serine," PNAS **104**, 20183–20188 (2007).

[16] B. Yan, S. Jaeqx, W. J. van der Zande, and A. M. Rijs, "A conformation-selective IR-UV study of the dipeptides Ac-Phe-Ser-NH_2 and Ac-Phe-Cys-NH_2: probing the SH···O and OH···O hydrogen bond interactions," Phys. Chem. Chem. Phys. **16**, 10770–10778 (2014).

[17] C. A. Taatjes, O. Welz, A. J. Eskola, J. D. Savee, A. M. Scheer, D. E. Shallcross, B. Rotavera, E. P. F. Lee, J. M. Dyke, D. K. W. Mok, D. L. Osborn, and C. J. Percival, "Direct measurement of conformer-dependent reactivity of the Criegee intermediate CH_3CHOO," Science **340**, 177 (2013).

[18] Y.-P. Chang, K. Długołęcki, J. Küpper, D. Rösch, D. Wild, and S. Willitsch, "Specific chemical reactivities of spatially separated 3-aminophenol conformers with cold Ca^+ ions," Science **342**, 98–101 (2013), arXiv:1308.6538 [physics].

[19] L. Khriachtchev, A. Domanskaya, K. Marushkevich, M. Räsänen, B. Grigorenko, A. Ermilov, N. Andrijchenko, and A. Nemukhin, "Conformation-dependent chemical reaction of formic acid with an oxygen atom," J. Phys. Chem. A **113**, 8143 (2009).

[20] H.-Y. Lin, Y.-H. Huang, X. Wang, J. M. Bowman, Y. Nishimura, H. A. Witek, and Y.-P. Lee, "Infrared identification of the Criegee intermediates *syn* and *anti*-CH_3CHOO, and their distinct conformation-dependent reactivity," Nat. Commun. **6**, 7012 (2015).

[21] R. Neutze, R. Wouts, D. van der Spoel, E. Weckert, and J. Hajdu, "Potential for biomolecular imaging with femtosecond X-ray pulses," Nature **406**, 752–757 (2000).

[22] M. M. Seibert, T. Ekeberg, F. R. N. C. Maia, M. Svenda, J. Andreasson, O. Jönsson, D. Odić, B. Iwan, A. Rocker, D. Westphal, M. Hantke, D. P. Deponte, A. Barty, J. Schulz, L. Gumprecht, N. Coppola, A. Aquila, M. Liang, T. A. White, A. Martin, C. Caleman, S. Stern, C. Abergel, V. Seltzer, J.-M. Claverie, C. Bostedt, J. D. Bozek, S. Boutet, A. A. Miahnahri, M. Messerschmidt, J. Krzywinski, G. Williams, K. O. Hodgson, M. J. Bogan, C. Y. Hampton, R. G. Sierra, D. Starodub, I. Andersson, S. Bajt, M. Barthelmess, J. C. H. Spence, P. Fromme, U. Weierstall, R. Kirian, M. Hunter, R. B. Doak, S. Marchesini, S. P. Hau-Riege, M. Frank, R. L. Shoeman, L. Lomb, S. W. Epp, R. Hartmann, D. Rolles, A. Rudenko, C. Schmidt, L. Foucar, N. Kimmel, P. Holl,

B. Rudek, B. Erk, A. Hömke, C. Reich, D. Pietschner, G. Weidenspointner, L. Strüder, G. Hauser, H. Gorke, J. Ullrich, I. Schlichting, S. Herrmann, G. Schaller, F. Schopper, H. Soltau, K.-U. Kühnel, R. Andritschke, C.-D. Schröter, F. Krasniqi, M. Bott, S. Schorb, D. Rupp, M. Adolph, T. Gorkhover, H. Hirsemann, G. Potdevin, H. Graafsma, B. Nilsson, H. N. Chapman, and J. Hajdu, "Single mimivirus particles intercepted and imaged with an x-ray laser," Nature **470**, 78 (2011).

[23] F. Filsinger, G. Meijer, H. Stapelfeldt, H. Chapman, and J. Küpper, "State- and conformer-selected beams of aligned and oriented molecules for ultrafast diffraction studies," Phys. Chem. Chem. Phys. **13**, 2076–2087 (2011), arXiv:1009.0871 [physics].

[24] A. Barty, J. Küpper, and H. N. Chapman, "Molecular imaging using x-ray free-electron lasers," Annu. Rev. Phys. Chem. **64**, 415–435 (2013).

[25] J. Küpper, S. Stern, L. Holmegaard, F. Filsinger, A. Rouzée, A. Rudenko, P. Johnsson, A. V. Martin, M. Adolph, A. Aquila, S. Bajt, A. Barty, C. Bostedt, J. Bozek, C. Caleman, R. Coffee, N. Coppola, T. Delmas, S. Epp, B. Erk, L. Foucar, T. Gorkhover, L. Gumprecht, A. Hartmann, R. Hartmann, G. Hauser, P. Holl, A. Hömke, N. Kimmel, F. Krasniqi, K.-U. Kühnel, J. Maurer, M. Messerschmidt, R. Moshammer, C. Reich, B. Rudek, R. Santra, I. Schlichting, C. Schmidt, S. Schorb, J. Schulz, H. Soltau, J. C. H. Spence, D. Starodub, L. Strüder, J. Thøgersen, M. J. J. Vrakking, G. Weidenspointner, T. A. White, C. Wunderer, G. Meijer, J. Ullrich, H. Stapelfeldt, D. Rolles, and H. N. Chapman, "X-ray diffraction from isolated and strongly aligned gas-phase molecules with a free-electron laser," Phys. Rev. Lett. **112**, 083002 (2014), arXiv:1307.4577 [physics].

[26] C. J. Hensley, J. Yang, and M. Centurion, "Imaging of isolated molecules with ultrafast electron pulses," Phys. Rev. Lett. **109**, 133202 (2012).

[27] J. Yang, M. Guehr, X. Shen, R. Li, T. Vecchione, R. Coffee, J. Corbett, A. Fry, N. Hartmann, C. Hast, K. Hegazy, K. Jobe, I. Makasyuk, J. Robinson, M. S. Robinson, S. Vetter, S. Weathersby, C. Yoneda, X. Wang, and M. Centurion, "Diffractive imaging of coherent nuclear motion in isolated molecules," Phys. Rev. Lett. **117**, 153002 (2016).

[28] F. Calegari, D. Ayuso, A. Trabattoni, L. Belshaw, S. De Camillis, S. Anumula, F. Frassetto, L. Poletto, A. Palacios, P. Decleva, J. B. Greenwood, F. Martín, and M. Nisoli, "Ultrafast electron dynamics in phenylalanine initiated by attosecond pulses." Science **346**, 336–339 (2014).

[29] F. J. Vastola and A. J. Pirone, "Ionization of organic solids by laser irradiation," Adv. Mass Spectrom. **4**, 107 (1968).

[30] A. M. Rijs and J. Oomens, eds., "IR spectroscopic techniques to study isolated biomolecules," in *Gas-Phase IR Spectroscopy and Structure of Biological Molecules* (Springer Verlag, 2015) Chap. 1, pp. 1–42.

[31] G. Meijer, M. S. de Vries, H. E. Hunziker, and H. R. Wendt, "Laser desorption jet-cooling of organic molecules – cooling characteristics and detection sensitivity," Appl. Phys. B **51**, 395–403 (1990).

[32] J. M. Bakker, L. M. Aleese, G. Meijer, and G. von Helden, "Fingerprint IR spectroscopy to probe amino acid conformations in the gas phase," Phys. Rev. Lett. **91**, 203003 (2003).

[33] N. Teschmit, K. Długołęcki, D. Gusa, I. Rubinsky, D. A. Horke, and J. Küpper, "Characterizing and optimizing a laser-desorption molecular beam source," J. Chem. Phys. **147**, 144204 (2017), arXiv:1706.04083 [physics].

[34] Y.-P. Chang, D. A. Horke, S. Trippel, and J. Küpper, "Spatially-controlled complex molecules and their applications," Int. Rev. Phys. Chem. **34**, 557–590 (2015), arXiv:1505.05632 [physics].

[35] F. Filsinger, U. Erlekam, G. von Helden, J. Küpper, and G. Meijer, "Selector for structural isomers of neutral molecules," Phys. Rev. Lett. **100**, 133003 (2008), arXiv:0802.2795 [physics].

[36] F. Filsinger, J. Küpper, G. Meijer, J. L. Hansen, J. Maurer, J. H. Nielsen, L. Holmegaard, and H. Stapelfeldt, "Pure samples of individual conformers: the separation of stereo-isomers of complex molecules using electric fields," Angew. Chem. Int. Ed. **48**, 6900–6902 (2009).

[37] J. H. Nielsen, P. Simesen, C. Z. Bisgaard, H. Stapelfeldt, F. Filsinger, B. Friedrich, G. Meijer, and J. Küpper, "Stark-selected beam of ground-state OCS molecules characterized by revivals of impulsive alignment," Phys. Chem. Chem. Phys. **13**, 18971–18975 (2011), arXiv:1105.2413 [physics].

[38] D. A. Horke, Y.-P. Chang, K. Długołęcki, and J. Küpper, "Separating para and ortho water," Angew. Chem. Int. Ed. **53**, 11965–11968 (2014), arXiv:1407.2056 [physics].

[39] S. Trippel, T. Mullins, N. L. M. Müller, J. S. Kienitz, R. González-Férez, and J. Küpper, "Two-state wave packet for strong field-free molecular orientation," Phys. Rev. Lett. **114**, 103003 (2015), arXiv:1409.2836 [physics].

[40] F. Filsinger, J. Küpper, G. Meijer, L. Holmegaard, J. H. Nielsen, I. Nevo, J. L. Hansen, and H. Stapelfeldt, "Quantum-state selection, alignment, and orientation of large molecules using static electric and laser fields," J. Chem. Phys. **131**, 064309 (2009), arXiv:0903.5413 [physics].

[41] Y.-P. Chang, F. Filsinger, B. Sartakov, and J. Küpper, "CMIstark: Python package for the stark-effect calculation and symmetry classification of linear, symmetric and asymmetric top wavefunctions in dc electric fields," Comp. Phys. Comm. **185**, 339–349 (2014), arXiv:1308.4076 [physics].

[42] L. Holmegaard, J. H. Nielsen, I. Nevo, H. Stapelfeldt, F. Filsinger, J. Küpper, and G. Meijer, "Laser-induced alignment and orientation of quantum-state-selected large molecules," Phys. Rev. Lett. **102**, 023001 (2009), arXiv:0810.2307 [physics].

[43] J. C. H. Spence and R. B. Doak, "Single molecule diffraction," Phys. Rev. Lett. **92**, 198102 (2004).

[44] M. Francl, "Zen and the art of molecules," Nat Chem **4**, 142–144 (2012).

[45] A third conformer was detected by the Mons group,[58] but with a population so minor that it is not considered in our study.

[46] G. von Helden, T. Wyttenbach, and M. T. Bowers, "Conformation of macromolecules in the gas-phase – use of matrix-assisted laser-desorption methods in ion chromatography," Science **267**, 1483–1485 (1995).

[47] F. Lanucara, S. W. Holman, C. J. Gray, and C. E. Eyers, "The power of ion mobility-mass spectrometry for structural characterization and the study of conformational dynamics," Nat. Chem. **6**, 281–294 (2014).

[48] V. Kumarappan, C. Z. Bisgaard, S. S. Viftrup, L. Holmegaard, and H. Stapelfeldt, "Role of rotational temperature in adiabatic molecular alignment," J. Chem. Phys. **125**, 194309 (2006).

[49] F. Filsinger, S. Putzke, H. Haak, G. Meijer, and J. Küpper, "Optimizing the resolution of the alternating-gradient m/μ selector," Phys. Rev. A **82**, 052513 (2010).

[50] J. S. Kienitz, K. Długołęcki, S. Trippel, and J. Küpper, "Improved spatial separation of neutral molecules," J. Chem. Phys. **147**, 024304 (2017), https://doi.org/10.1063/1.4991479.

[51] S. Trippel, M. Johny, T. Kierspel, J. Onvlee, H. Bieker, H. Ye, T. Mullins, L. Gumprecht, K. Długołęcki, and J. Küpper, "Knife edge skimming for improved separation of molecular species by the deflector," (2018), submitted, arXiv:1802.04053 [physics].

[52] U. Even, J. Jortner, D. Noy, N. Lavie, and N. Cossart-Magos, "Cooling of large molecules below 1 K and He clusters formation," J. Chem. Phys. **112**, 8068–8071 (2000).

[53] S. Trippel, Y.-P. Chang, S. Stern, T. Mullins, L. Holmegaard, and J. Küpper, "Spatial separation of state- and size-selected neutral clusters," Phys. Rev. A **86**, 033202 (2012), arXiv:1208.4935 [physics].

[54] W. Ackermann, G. Asova, V. Ayvazyan, A. Azima, N. Baboi, J. Bähr, V. Balandin, B. Beutner, A. Brandt, A. Bolzmann, R. Brinkmann, O. I. Brovko, M. Castellano, P. Castro, L. Catani, E. Chiadroni, S. Choroba, A. Cianchi, J. T. Costello, D. Cubaynes, J. Dardis, W. Decking, H. Delsim-Hashemi, A. Delserieys, G. Di Pirro, M. Dohlus, S. Düsterer, A. Eckhardt, H. T. Edwards, B. Faatz, J. Feldhaus, K. Flöttmann, J. Frisch, L. Fröhlich, T. Garvey, U. Gensch, C. Gerth, M. Görler, N. Golubeva, H. J. Grabosch, M. Grecki, O. Grimm, K. Hacker, U. Hahn, J. H. Han,

K. Honkavaara, T. Hott, M. Hüning, Y. Ivanisenko, E. Jaeschke, W. Jalmuzna, T. Jezynski, R. Kammering, V. Katalev, K. Kavanagh, E. T. Kennedy, S. Khodyachykh, K. Klose, V. Kocharyan, M. Körfer, M. Kollewe, W. Koprek, S. Korepanov, D. Kostin, M. Krassilnikov, G. Kube, M. Kuhlmann, C. L. S. Lewis, L. Lilje, T. Limberg, D. Lipka, F. Löhl, H. Luna, M. Luong, M. Martins, M. Meyer, P. Michelato, V. Miltchev, W. D. Möller, L. Monaco, W. F. O. Müller, O. Napieralski, O. Napoly, P. Nicolosi, D. Nölle, T. Nuñez, A. Oppelt, C. Pagani, R. Paparella, N. Pchalek, J. Pedregosa-Gutierrez, B. Petersen, B. Petrosyan, G. Petrosyan, L. Petrosyan, J. Pflüger, E. Plönjes, L. Poletto, K. Pozniak, E. Prat, D. Proch, P. Pucyk, P. Radcliffe, H. Redlin, K. Rehlich, M. Richter, M. Roehrs, J. Roensch, R. Romaniuk, M. Ross, J. Rossbach, V. Rybnikov, M. Sachwitz, E. L. Saldin, W. Sandner, H. Schlarb, B. Schmidt, M. Schmitz, P. Schmüser, J. R. Schneider, E. A. Schneidmiller, S. Schnepp, S. Schreiber, M. Seidel, D. Sertore, A. V. Shabunov, C. Simon, S. Simrock, E. Sombrowski, A. A. Sorokin, P. Spanknebel, R. Spesyvtsev, L. Staykov, B. Steffen, F. Stephan, F. Stulle, H. Thom, K. Tiedtke, M. Tischer, S. Toleikis, R. Treusch, D. Trines, I. Tsakov, E. Vogel, T. Weiland, H. Weise, M. Wellhöfer, M. Wendt, I. Will, A. Winter, K. Wittenburg, W. Wurth, P. Yeates, M. V. Yurkov, I. Zagorodnov, and K. Zapfe, "Operation of a free-electron laser from the extreme ultraviolet to the water window," Nat. Photon. **1**, 336–342 (2007).

[55] T. Kierspel, J. Wiese, T. Mullins, J. Robinson, A. Aquila, A. Barty, R. Bean, R. Boll, S. Boutet, P. Bucksbaum, H. N. Chapman, L. Christensen, A. Fry, M. Hunter, J. E. Koglin, M. Liang, V. Mariani, A. Morgan, A. Natan, V. Petrovic, D. Rolles, A. Rudenko, K. Schnorr, H. Stapelfeldt, S. Stern, J. Thøgersen, C. H. Yoon, F. Wang, S. Trippel, and J. Küpper, "Strongly aligned molecules at free-electron lasers," J. Phys. B **48**, 204002 (2015), arXiv:1506.03650 [physics].

[56] M. S. Gordon and M. W. Schmidt, "Advances in electronic structure theory: Gamess a decade later," in *Theory and Applications of Computational Chemistry: the first forty years*, edited by C. E. Dykstra, G. Frenking, K. S. Kim, and G. E. Scuseria (Elsevier, Amsterdam, 2005).

[57] S. Stern, L. Holmegaard, F. Filsinger, A. Rouzée, A. Rudenko, P. Johnsson, A. V. Martin, A. Barty, C. Bostedt, J. D. Bozek, R. N. Coffee, S. Epp, B. Erk, L. Foucar, R. Hartmann, N. Kimmel, K.-U. Kühnel, J. Maurer, M. Messerschmidt, B. Rudek, D. G. Starodub, J. Thøgersen, G. Weidenspointner, T. A. White, H. Stapelfeldt, D. Rolles, H. N. Chapman, and J. Küpper, "Toward atomic resolution diffractive imaging of isolated molecules with x-ray free-electron lasers," Faraday Disc. **171**, 393 (2014), arXiv:1403.2553 [physics].

[58] M. Alauddin, H. S. Biswal, E. Gloaguen, and M. Mons, "Intra-residue interactions in proteins: interplay between serine or cysteine side chains and backbone conformations, revealed by laser spectroscopy of isolated model peptides," Phys. Chem. Chem. Phys. **17**, 2169–2178 (2015).